
www.palgrave-journals.com/jos/

Simulation and enhancement of a cardiovascular device test rig

SD Gregory[1,2]*, N Greatrex[1,2], D Timms[2], N Gaddum[1], MJ Pearcy[1] and JF Fraser[2]

[1]*Queensland University of Technology, Brisbane, Australia; and* [2]*The Prince Charles Hospital, Brisbane, Australia*

Cardiovascular assist devices are tested in mock circulation loops (MCLs) prior to animal and clinical testing. These MCLs rely on characteristics such as pneumatic parameters to create pressure and flow, and pipe dimensions to replicate the resistance, compliance and fluid inertia of the natural cardiovascular system. A mathematical simulation was developed in SIMULINK to simulate an existing MCL. Model validation was achieved by applying the physical MCL characteristics to the simulation and comparing the resulting pressure traces. These characteristics were subsequently altered to improve and thus predict the performance of a more accurate physical system. The simulation was successful in simulating the physical MCL, and proved to be a useful tool in the development of improved cardiovascular device test rigs.
Journal of Simulation (2010) **4,** 34–41. doi:10.1057/jos.2009.15

Keywords: engineering; medicine; simulation; mock circulation loop; cardiovascular devices

1. Introduction

With approximately one in five people in the United States developing some degree of heart failure in their lifetime, and a limited number of donor hearts available, a mechanical solution is often required (Lloyd-Jones *et al*, 2002; Scherr *et al*, 2004; Selzman *et al*, 2006; Vitali *et al*, 2004). An encouraging solution to this donor shortage appears to be in the form of Ventricular assist devices (VADs), which are used to assist and unload a patient's failing heart. VADs can also be used as a destination therapy for patients who are not transplant candidates.

Several designs of VADs are commercially available or under development. Before expensive animal or human trials are conducted, mock circulation loops (MCLs) are employed to test these assist devices to assess and improve their performance. MCLs are also required to comply with US Food and Drug Administration regulations, but are not intended to replace *in-vivo* trials (Patel *et al*, 2003; Timms *et al*, 2005). MCLs are also used as a mechanical representation of the human cardiovascular system for *in-vitro* testing of artificial heart valves, total artificial hearts, aortic balloon pumps and almost any other cardiovascular device.

An MCL is required to accurately represent the natural characteristics of the human cardiovascular system. The pulsatile nature of the atria and ventricles, the vascular resistance, fluid inertia and compliance of the blood vessel walls must be accurately represented. Pressures, flows and fluid volumes in each segment of the body must be accurately replicated in the MCL.

Previous MCL designs vary from simple systems consisting of a constant flow pre-load chamber and resistance valve, to complex systems that accurately represent the resistance, compliance, fluid inertia and pulsatile nature of the natural cardiovascular system. The design of the MCL analyzed in this study has been presented previously (Timms *et al*, 2005). This system uses proportional valves to represent lumped vascular resistance, trapped volumes of air to represent lumped compliance and the fluid volume in the piping to represent inertiance. A mathematical simulation was developed to model this physical system and improve the resulting pressure and flow traces by changing the represented physical characteristics of the system.

Several simulations of the cardiovascular system have been presented previously. An earlier simulation known as PHYSBE provided a lumped parameter, nonlinear system to represent the flow of blood, and its properties such as heat, throughout the circulatory system (Korn *et al*, 1970). This simulation was later converted into a SIMULINK model. Resistance, compliance, blood volume and flow are all included in this model; however, the inertia of the fluid is not.

An advanced model of the circulatory system including an artificial heart was developed by Ding and Frank (1994). This system included resistance, compliance and inertiance, while also developing complex reflex control systems such as the baroreceptor response and nonlinear vessel compliance.

A concentrated parameter model of the complete circulation was developed by Korakianitis and Shi (2006) to study the dynamic function of the human circulation. This study used magnetic resonance imaging technology to obtain

*Correspondence: SD Gregory, GPO Box 2434, Brisbane, QLD 4001, Australia.
E-mail: shaun.gregory@qut.edu.au

Glossary

A	Cross sectional area of pipe
C	Compliance
g	Gravitational constant
K_a	Bulk modulus of air
l	Length
L	Inertiance
m	Mass of fluid
m_a	Mass of air
MCL	Mock circulation loop
MRI	Magnetic resonance imaging
P_a	Air pressure in compliance chamber
P_c	Fluid pressure in compliance chamber
P_{inlet}	Subsystem inlet pressure
P_{outlet}	Subsystem outlet pressure
p_{reg}	Density of air from regulator
P_{reg}	Pressure of air from regulator
Q_c	Flow rate of fluid into compliance chamber
Q_{inlet}	Subsystem inlet flow rate
Q_{outlet}	Subsystem outlet flow rate
r	Radius
R	Resistance
r_h	Radius of horizontal pipe
R_{reg}	Resistance of regulator tubing
t	Time
V_a	Volume of air
VAD	Ventricular assist devices
$V_c(0)$	Initial fluid volume in compliance chamber
$\ddot{x}$	Acceleration of centre of mass of fluid
$\tilde{n}_c$	Density
μ	Fluid viscosity

ventricle shapes and suitable inputs to the numerical models. The ventricles were modelled by using a variable elastance, while the heart valves were modelled to include features such as pressure differences, frictional forces and vortex effects. Resistance, compliance and inertiance were also incorporated in this model.

Cardiovascular system models have also been created by other groups (Vollkron *et al*, 2002; Wu *et al*, 2003; Vrettos, 2005; Hassani *et al*, 2007), however, the mentioned simulations concentrate solely on the cardiovascular system, and do not provide an accurate representation of an MCL.

The aim of this study was to create and validate a mathematical simulation of an existing MCL, and use this simulation to design an improved physical MCL system.

2. Methods

2.1. Mathematical modelling

The MCL approximates the haemodynamics of the human cardiovascular system by using lumped equivalent hydraulic components. A layout of the MCL is shown in Figure 1.

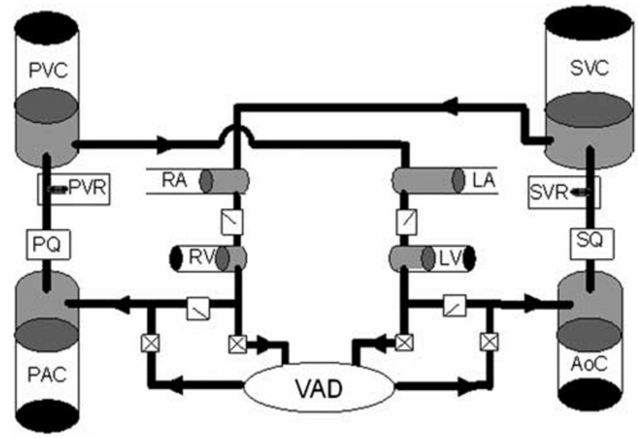

Figure 1 Layout of the physical Mock Circulation Loop. Compliance chambers, variable resistance valves, one-way valves and connections to the prototype VADs are all shown.

The MCL consists of a number of components including rigid pipes, linear and nonlinear compliance chambers, one-way valves and variable resistance valves. Equations describing the flow and pressure characteristics of linear resistances, linear compliance chambers and fluid inertiance are well understood and were used to develop a set of simultaneous differential equations. All terms are defined in the glossary. Parameters for the various components were determined from equations (1)–(3).

Resistance (R) and fluid inertia (L) values for a section of rigid pipe is given by

$$R = 8 \cdot \mu \cdot \pi \cdot \frac{1}{(\pi \cdot r^2)^2} \tag{1}$$

$$L = \rho_c \cdot \frac{l}{\pi \cdot r_h^2} \tag{2}$$

The compliance (C) value for the linear compliance chambers are given as

$$C = \frac{A}{\rho_c \cdot g} \tag{3}$$

2.2. Ventricular and atrial compliance chambers

Unlike the compliance chambers for the systemic and pulmonary systems, the ventricular and atrial compliance chambers have a variable compliance that can be adjusted using air pressure. The existing MCL uses air regulators, which produce unphysiologic square pressure waves through solenoid valves, to adjust the air pressure above the fluid volume to create higher or lower levels of compliance. Periodic pressure changes in the air produce a contractility function similar to the natural heart. Figure 2 shows a diagram of the compliance chamber and its associated variables.

Gravitational forces, pressure differences and compression of the regulated air all contribute to the effective compliance

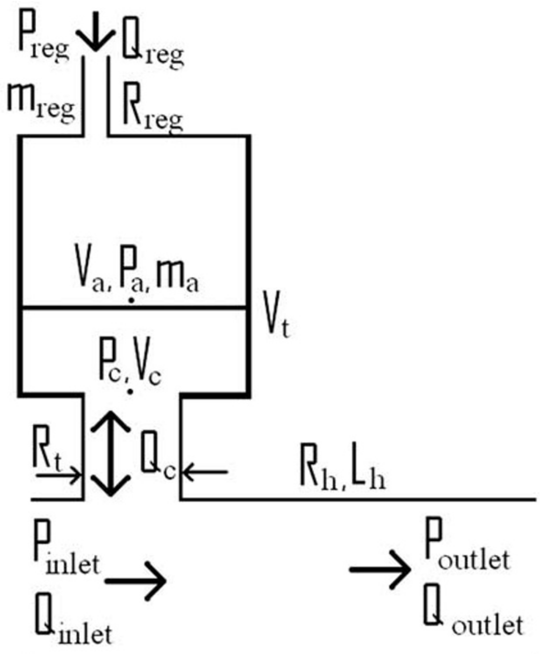

Figure 2 Parameters in each subsystem of mock circulation loop simulation. P—pressure, m—mass, Q—flow rate, R—resistance, V—volume, L—fluid inertia, reg—regulator, a—air, c—compliance chamber fluid, t—compliance chamber entry pipe, inlet—input to system, outlet—output from system.

of the chamber. The free body diagram shown in Figure 3 indicates the gravitational and pressure forces that are acting on the body of fluid in the chamber. Equation (4) shows the sum of forces for this system.

$$P_c \cdot A - mg - P_a \cdot A = m \cdot \ddot{x} \tag{4}$$

Both the mass and acceleration of the fluid can be written in terms of the flow into the chamber and are shown in equation (5) and (6). The acceleration of fluid into the compliance chambers must be divided by two as this is taken at the centre of mass, rather than the top of the chamber fluid.

$$\ddot{x} = \frac{1}{2A} \cdot \frac{dQ_c}{dt} \tag{5}$$

$$m = \rho_c(V_c(0) + \int Q_c\, dt) \tag{6}$$

Substituting and rearranging equations (5) and (6) into (4) gives

$$P_c = \frac{\rho_c}{2A^2} \cdot \frac{dQ_c}{dt} \cdot (V_c(0) + \int Q_c\, dt) + \rho_c \cdot \frac{g}{A} \cdot (V_c(0) + \int Q_c\, dt) + P_a \tag{7}$$

Equation (7) contains three terms that contribute to the compliance pressure. The first term is a nonlinear inertiance

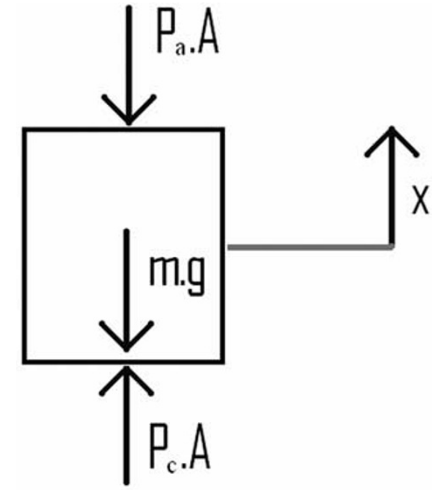

Figure 3 Free body diagram of fluid in vertical chamber. P_a—air pressure, A—cross sectional area of fluid body, m—mass, g—gravitational constant, P_c—fluid pressure, x—displacement of centre of mass of fluid body.

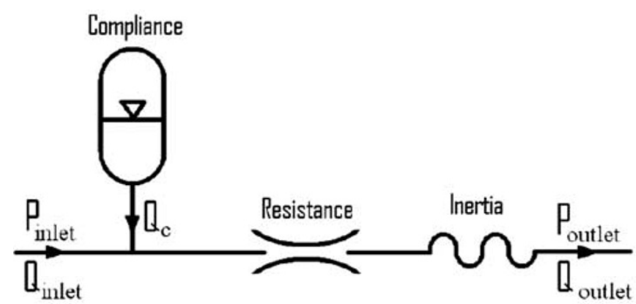

Figure 4 Base subsystem of the simulation. Each subsystem consists of a compliance, resistance and inertiance element.

function that affects the pressure when large changes in input flow are present. The second term is the compliance component that is related to the gravitational potential energy stored in the body of fluid. The final term accounts for the contribution from the pressure of the air above the body of fluid. Assuming constant temperature, the pressure of air in the chamber is dependent on the initial mass and volume of air in the chamber and the mass of air injected by the regulator. Using the bulk modulus of air and ideal gas law a function for the air pressure can be derived and is shown in equation (8).

$$\frac{dP_a}{dt} + \frac{K_a \rho_{reg}}{R_{reg} m_a} P_a = K_a \left(\frac{\rho_{reg} P_{reg}}{R_{reg} m_a} + \frac{Q_c}{V_a} \right) \tag{8}$$

2.3. Simulation methodology

Due to the MCL's circular topology, individual sections of the loop were grouped into subsystems and linked in series.

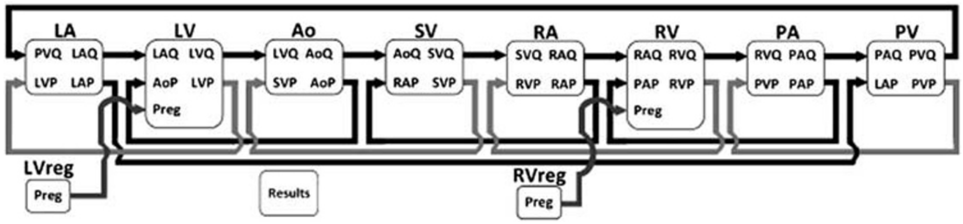

Figure 5 Linked subsystems in mock circulation loop simulation. From left to right in top row—Left atrium, left ventricle, systemic arterial, systemic venous, right atrium, right ventricle, pulmonary arterial and pulmonary venous subsystems. From left to right in bottom row—left ventricle regulator, results and right ventricle regulator subsystems.

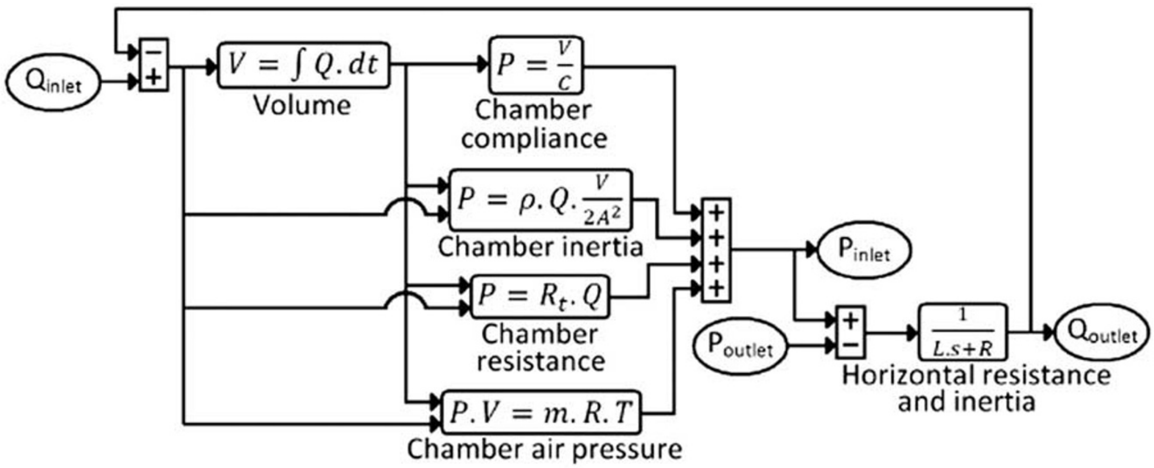

Figure 6 Flow diagram of subsystem. Inputs Q_{inlet} and P_{outlet} produce outputs Q_{outlet} and P_{inlet}. Ventricle subsystems include a regulator block in place of the chamber air pressure block.

Each subsystem has an identical structure and only differ with the parameter values. Figure 4 shows the structure of the base subsystem.

Ventricle and atrium subsystems have an identical structure as the base subsystems, but include a one-way valve and the nonlinear compliance function outlined in equation (7). The mechanical check valves used in the MCL to simulate the natural heart valves were modelled using a saturation block with an infinite upper flow limit and a lower flow limit of zero to prevent backflow.

Each of these subsystems has four variables associated with it; input flow and pressure and output flow and pressure. The inlet flow and outlet pressure were chosen to be independent, while the remaining two variables became dependent. As such, each subsystem is a function of the previous and next subsystem. The topology of the simulation's subsystems is shown in Figure 5.

Kirchhoff's junction rule is used to determine the pressure at the inlet of the compliance chamber. The output flow is determined from the known outlet pressure and the calculated inlet pressure. Equations (9) and (10) show the coupled differential equations that are solved to find the two dependent variables. Equation (11) shows the state space representation of the system of equation that are implemented in SIMULINK. A flow diagram of the subsystem is shown in Figure 6.

$$C\frac{dP_{\text{inlet}}}{dt} = Q_{\text{compliance}} = Q_{\text{inlet}} - Q_{\text{outlet}} \tag{9}$$

$$L\frac{dQ_{\text{outlet}}}{dt} + RQ_{\text{outlet}} = P_{\text{outlet}} - P_{\text{inlet}} \tag{10}$$

$$\begin{bmatrix} \frac{dP_{\text{inlet}}}{dt} \\ \frac{dQ_{\text{outlet}}}{dt} \end{bmatrix} = \begin{bmatrix} 0 & -\frac{1}{c} \\ -\frac{1}{L} & -\frac{R}{L} \end{bmatrix} \begin{bmatrix} P_{\text{inlet}} \\ Q_{\text{outlet}} \end{bmatrix} + \begin{bmatrix} \frac{1}{C}Q_{\text{inlet}} \\ \frac{1}{L}P_{\text{outlet}} \end{bmatrix} \tag{11}$$

2.4. Stability

The system of differential equations derived for the simulation are inherently stiff for some parameter values. Caution must be taken when determining the parameter values, as small parameter variations can have significant effects on the simulation's stability. The stiff DE solver ode23s was used in SIMULINK to solve the simulation.

In particular, the derivative component in equation (7) introduces instability and algebraic loops into the simulation. To alleviate these problems, the differentiator was implemented with an additional second-order low-pass filter. The cutoff frequency of the low-pass filter was chosen to be much higher than the fundamental frequencies of the simulation so the effects are minimal. The addition of the low-pass filter significantly reduced the instability of the simulation without any noticeable effect on the solution.

2.5. Model validation

The physical characteristics from the existing MCL, such as pipe dimensions and regulator pressures, were applied to the simulation (Table 1). A healthy, resting condition was simulated using the parameters obtained from the physical system. A left heart failure situation was also reproduced in the simulation by altering the ventricle regulator pressures, vascular resistances and arterial compliance. Pressure and flow traces produced by the simulation were then compared to those seen in the physical system.

Table 1 Parameters used in the mock circulation loop simulation to simulate healthy rest and left heart failure conditions

	Rest	*Left Heart failure*
SVR radius (mm)	1.01	0.95
PVR radius (mm)	2.2	2.2
Left ventricle regulator pressure (mmHg)	122	65
Right ventricle regulator pressure (mmHg)	26	41
Aorta l_p (mm) (Ao Compliance)	190	100
Pulmonary artery l_p (mm) (PA Compliance)	450	240

SVR—Systemic vascular resistance, PVR—Pulmonary vascular resistance, l_p—Total length of pipe in compliance chamber, Ao—Aorta, PA—Pulmonary artery.

2.6. Simulation improvements

Pipe dimensions and input parameters, such as regulator pressures, were adjusted through trial and error to achieve more haemodynamically accurate pressure and flow waveforms and magnitudes. Simulated left atrial systole was added to represent the natural heart with greater accuracy. A pulse duration of 0.2 s was supplied to accurately represent atrial systole at 60 beats per minute (20% of the cardiac cycle). The resulting pressure and flow traces produced by the simulation were then compared to cases seen in the literature for natural pressure and flow traces.

A pressure pulse for 40% of the cardiac cycle simulated ventricular systole, and occurred at a phase delay of 20% of the cardiac cycle (0.2 s) after the onset of atrial systole. These ventricle pressure pulses were physiologically improved by varying the magnitude of pulse pressure from the ventricle regulator (ITV2030-012BS5, SMC Pneumatics, Brisbane, Australia) at 0.1 s intervals throughout the ventricular systolic phase.

3. Results

Results were obtained to ensure the simulation could provide an accurate representation of the physical MCL.

3.1. Simulation model validation

Pressure traces produced by the simulation were shown to closely represent those seen in the physical system for both the systemic (Figure 7) and pulmonary (Figure 8) sides under healthy resting and left heart failure conditions. The oscillations in the ventricle pressure traces from the physical system, due to water hammer, were not replicated in the simulation. The aortic and pulmonary arterial pressure waves peaked earlier in the simulation compared to the physical system. Results from this simulation were then used to optimize the model to more closely replicate the results from the physical system.

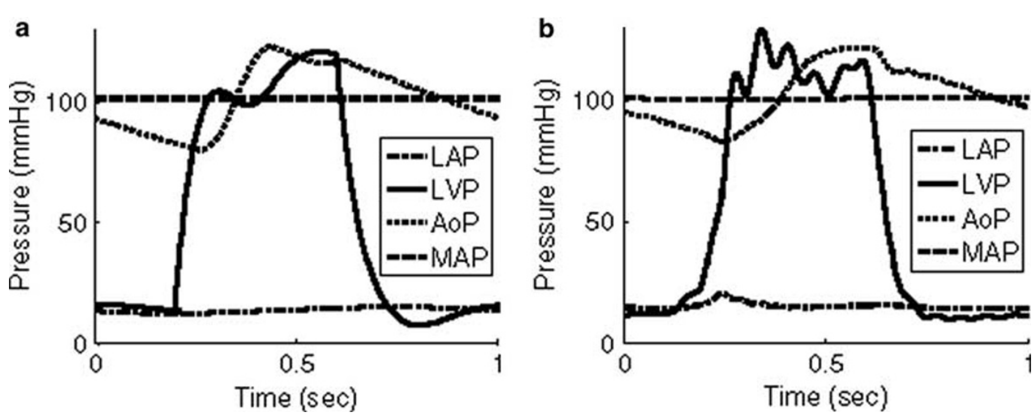

Figure 7 Comparison of systemic pressure traces between (a) MCL simulation, and (b) physical MCL. LAP—Left atrial pressure, LVP—Left ventricle pressure, AoP—Aortic pressure, MAP—Mean aortic pressure.

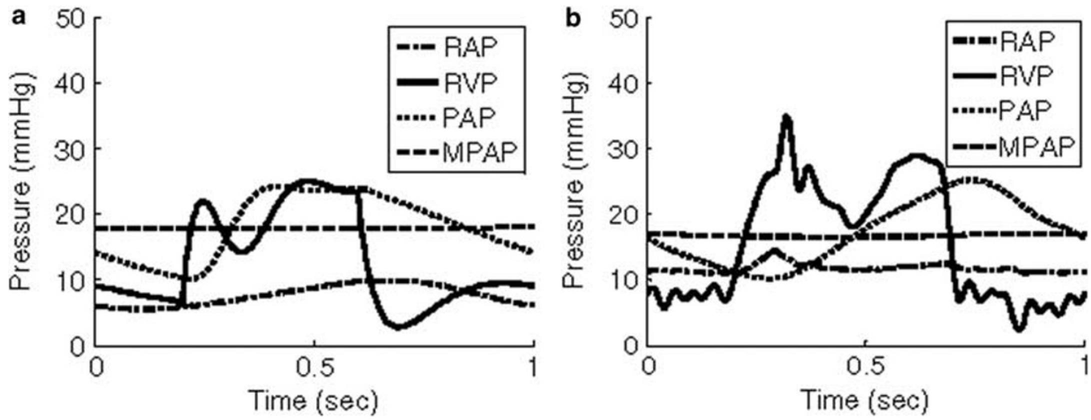

Figure 8 Comparison of pulmonary pressure traces between (a) MCL simulation, and (b) physical MCL. RAP—Right atrial pressure, RVP—Right ventricle pressure, PAP—Pulmonary artery pressure, MPAP—Mean pulmonary artery pressure.

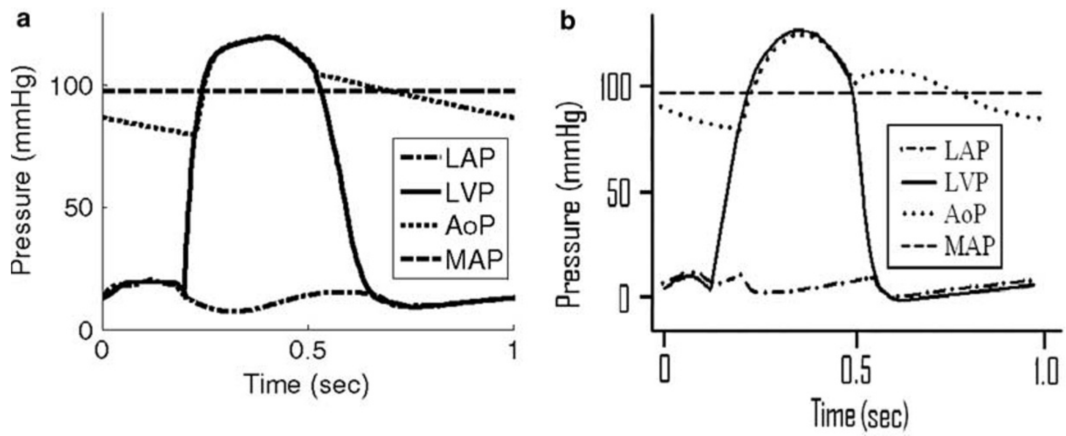

Figure 9 Comparison of systemic pressure traces between (a) optimized MCL simulation, and (b) natural systemic pressure trace. LAP—Left atrial pressure, LVP—Left ventricle pressure, AoP—Aortic pressure, MAP—Mean aortic pressure.

Table 2 Comparison of optimized MCL simulation haemodynamics to a natural, healthy situation (Hurst *et al*, 1974)

	MCL model	*Healthy adult male*
LVP (mmHg)	8–120	7–120
AoP (mmHg)	80–120	80–120
MAP (mmHg)	97	95
LAP (mmHg)	8–20	3–13
SQ (L/min)	5	5
RVP (mmHg)	4–25	4–25
PAP (mmHg)	10–25	10–25
MPAP (mmHg)	18	15
RAP (mmHg)	5–9	2–7
RQ (L/min)	5	5

LVP—Left ventricle pressure, AoP—Aortic pressure, MAP—Mean aortic pressure, LAP—Left atrial pressure, SQ—Systemic flow, RVP—Right ventricle pressure, PAP—Pulmonary arterial pressure, MPAP—Mean pulmonary arterial pressure, RAP—Right atrial pressure, RQ—Pulmonary flow rate.

3.2. Simulation model enhancement

The enhanced simulation produced far more haemodynamically accurate pressure waveforms (Figure 9) compared to the previous simulation. Pressure and flow magnitudes of the improved simulation (Table 2) remained similar to those seen in the previous simulation; however, the shapes of the curves were significantly altered.

4. Discussion

Dynamic performance of a system is often neglected in the design phase due to the expense and the time required. Using simulation packages, process systems can be evaluated in a small amount of time and at a low cost. Gonzalez-Bustamante *et al* (2007) stated that reasons for simulating a system were the design of regulation and control systems, and to predict the performance of the system. A simulation must include all components that have any effect on the dynamic behaviour of the system, while also being able to change model parameters that may influence the system. State equations and mass, momentum and energy conservation principles must be followed. Assumptions can be made in the simulation providing only a negligible effect is given, such as one-dimensional flow through a system. Validation of the simulation can be performed by comparing the results using other recognized software, or by those of a similar physical system. Adjustment of different input parameters resulted in variation of the pressure, flow and volume outputs of the system. Increased ventricle contractility resulted in increased pressures and flow rates and decreased ventricle volumes, while increased resistance lead to higher pressures and lower flow rates. Reduced distance between adjoining subsystems resulted in a shorter pressure and flow phase lag between the subsystems, producing more haemodynamically accurate results.

4.1. Model validation

The methods used to model the physical MCL using equations for pressure and flow provided an accurate representation of the system. The input parameters of pipe dimensions, regulator pressures and a series of constants allowed simple manipulation of the simulation. Adjustment of different input parameters resulted in variation of the pressure, flow and volume outputs of the system. Increased ventricle contractility resulted in increased pressures and flow rates and decreased ventricle volumes, while increased resistance led to higher pressures and lower flow rates. Reduced distance between adjoining subsystems resulted in a shorter pressure and flow phase lag between the subsystems, producing more haemodynamically accurate results.

Comparison of results produced by the first simulation and the physical system showed some correlation but there were differences in some parameters. The ventricle pressures in the physical system showed double pulses in the pulmonary circulation; however, these were not present in the systemic circulation. This double pulse can be eliminated by reducing the length between the ventricle and arterial subsystem in the simulation, indicating that the impedance of the ventricle is not correct in the simulation. The impedances of the model atria and arterial systems also appear to have a slight discrepancy, with the simulated arterial pressures peaking too early and the ventricle pressures dipping during the start of diastole. Notches due to valve closure can be observed in the simulation results. However, they are not of the same magnitude as that seen in the physical system. This is due to the heavy physical check valves being modelled as perfect valves.

To improve the accuracy of this simulation, pressure losses due to elbows and tee sections in the physical system must be represented in the simulation. The heavy mechanical check valves must be modelled with improved accuracy to produce the small oscillations present in the pressure traces from the physical system.

4.2. Model enhancement

The simulation was enhanced by changing pipe dimensions, adding an atrial systole and adding a variable ventricle regulator pressure. Heart chambers and arterial systems were moved closer together to improve the impedance between the systems. A markedly improved pressure waveform was observed for all pressures recorded in the simulation, while magnitudes of both pressure and flow were kept consistent with natural values reported in the literature. Slight discrepancies were observed between the pressure magnitudes of the improved simulation and those of a natural healthy male. Both systemic and pulmonary atrial pressures were higher in the simulation than those seen in natural cases, indicating a lower venous resistance in the simulation. Although systolic and diastolic arterial pressures are equal in both the aorta and pulmonary artery with natural values, mean arterial pressures recorded higher values in the simulation than the natural case. This can be attributed to the haemodynamically inaccurate linear diastolic arterial pressure waveforms compared to the curved natural pressure waveforms.

Natural pressure traces in the atria produce a notch following mitral valve closure due to the ventricle pushing into the atrium during systole. A small notch is produced in the simulation due to valve closure; however, the magnitude of the natural atrial notch cannot be replicated due to the physical system consisting of rigid pipes. Replacing the rigid ventricles and atria with compliant materials in the physical system could improve this result.

5. Conclusion

A mathematical simulation of a MCL was developed that provided an accurate representation of a previously developed physical system. Modelling in the MATLAB/SIMULINK environment allowed for simple simulation manipulation and data recording. The simulation was successfully developed to produce haemodynamically accurate pressure and flow waveforms. Using the results obtained from this simulation, a more accurate physical MCL can be constructed, thus reducing the number of expensive animal and clinical trials required to validate cardiovascular assist devices.

References

Ding X and Frank PM (1994). Modelling, control and monitoring of circulatory systems with an artificial heart. *Int J Qual Reliab Mngt* **11**: 41–50.

Gonzalez-Bustamante JA *et al* (2007). Modelling and dynamic simulation of processes with 'MATLAB'. An application of a natural gas installation in a power plant. *Energy* **32**: 1271–1282.

Hassani K, Navidbakhsh M and Rostami M (2007). Modeling of the aorta artery aneurysms and renal artery stenosis using cardiovascular electronic system. *BioMed Eng OnLine* **6**, 22doi:10.1186/1475-925X-6-22.

Hurst J, Logue R, Schlant R and Wenger N (1974). *The Heart*. McGraw-Hill: USA.

Korakianitis T and Shi Y (2006). A concentrated parameter model for the human cardiovascular system including heart valve dynamics and atrioventricular interaction. *Med Eng Phys* **28**: 613–628.

Korn G, Mcleod J and Wait J (1970). Dare/Physbe. *SIMULATION* **15**: 229–231.

Lloyd-Jones D *et al* (2002). Lifetime risk for developing congestive heart failure: The Framingham Heart Study. *Circulation* **106**: 3068–3072.

Patel S *et al* (2003). Design and construction of a mock human circulatory system. *Summer bioengineering conference* , June 25–29, pp 965–966.

Scherr K, Jensen L and Koshal A (2004). Characteristics and outcomes of patients bridged to cardiac transplantation on centrifugal ventricular assist devices: A case series of the early experience of one Canadian transplant centre. *Eur J Cardiovasc Nurs* **3**: 173–181.

Selzman C *et al* (2006). Surgical therapy for heart failure. *J Am Coll Surg* **203**: 226–239.

Timms D, Hayne M, Mcneil K and Galbraith A (2005). A complete mock circulation loop for the evaluation of left, right, and biventricular assist devices. *Artif Organs* **29**: 564–572.

Vitali E *et al* (2004). Mechanical circulatory support in severe heart failure: Single-center experience. *Transplant P* **36**: 620–622.

Vollkron M, Schima H, Huber L and Wieselthaler G (2002). Interaction of the cardiovascular system with an implanted rotary assist device: Simulation study with a refined computer model. *Artif Organs* **24**: 349–359.

Vrettos A (2005). The importance of arterial compliance, when blood flows and pressures are assumed to be random processes. *The Twenty-Fourth IASTED International Conference On Modelling, Identification and Control,* Innsbruck, Austria.

Wu Y *et al* (2003). An advanced physiological controller design for a left ventricular assist device to prevent left ventricular collapse. *Artif Organs* **27**: 926–930.

Received 31 October 2008; accepted 10 June 2009